The Hierarchical Origin of Galaxy Morphologies

Matthias Steinmetz

Steward Observatory, 933 N Cherry Ave, Tucson AZ, USA

Abstract

I review recent progress in numerically simulating the formation and evolution of galaxies. Special emphasis is given to results based on high resolution gas dynamical simulations that incorporate the effects of star formation and related feedback processes. Applications address the origin of galaxy morphologies and the properties of high redshift galaxies. Connections between the population of high redshift galaxies and Lyα absorption systems are drawn.

1 Introduction

The past couple of years have witnessed a tremendous advancement in the observational study of galaxy formation and evolution. While even a few years ago observational studies of galaxy evolution were restricted to redshifts substantially below one, nowadays properties of galaxies are routinely investigated at redshifts exceeding three (Steidel et al. 1996). The population of high-z galaxies, also called Lyman-break galaxies (henceforth LBG), are relatively bright (about L_*), abundant (comoving densities similar to present day L_* galaxies) and relatively compact (sizes corresponding to a few kpc). Multi–wavelength studies indicate that dust absorption may be of considerable importance, with typical values corresponding to an obscuration of about 1.5 magnitudes at a restframe wavelength of 1500 Å (Steidel, Pettini & Adelberger 2001).

Theoretical studies of properties of LBGs and their clustering have been performed using analytical (e.g. Mo & Fukushita 1996), semi analytical (Baugh et al. 1998, Kauffmann et al. 1999, Somerville, Primack & Faber 2001) and numerical work (e.g. Contardo, Steinmetz & Fritze-von Alvensleben 1998, Katz, Weinberg & Hernquist 1999, Pearce et al. 1999), mainly in the context of hierarchical clustering scenarios such as the well known cold dark matter (CDM) model (see, however, Bouwens, Broadhurst & Silk 1999). Those studies indicate that, at least on a qualitative level, the properties and clustering of Lyman-break galaxies can be well understood if LBGs are considered to represent the high luminosity end of the high-z luminosity function. This interpretation indicates that LBGs are the progenitors of the most massive galaxies which can be found in galaxy clusters today, while the progenitors of typical field and group galaxies such as the Milky Way fall above the magnitude limit of about 25.5 (i.e. they are too dim). This suggestion has been confirmed by the hybrid numerical/analytical study of Haehnelt, Steinmetz & Rauch (2000) which indicated that more than 80% of the protogalactic clumps (PGCs) at redshift three which are capable of producing damped Lyman alpha absorption fall above the magnitude limit of spectroscopic surveys, i.e. they are too dim to be identified with the population of Lyman break galaxies. In an alternative scenario, Somerville et al. (2001) proposed that LBGs typically correspond to less massive galaxies that are brightened by starbursts.

The hierarchical build-up is also thought to determine the morphology of a galaxy, most noticeably the difference between disk like systems such as spiral galaxies (some of them barred) and spheroidal systems such as elliptical galaxies and bulges. This picture envisions that whenever gas

"Dwarf Galaxies and their Environment"; Bad Honnef, Germany, 23-27 January 2001; Eds. K.S. de Boer, R.-J.Dettmar, U. Klein; Shaker Verlag

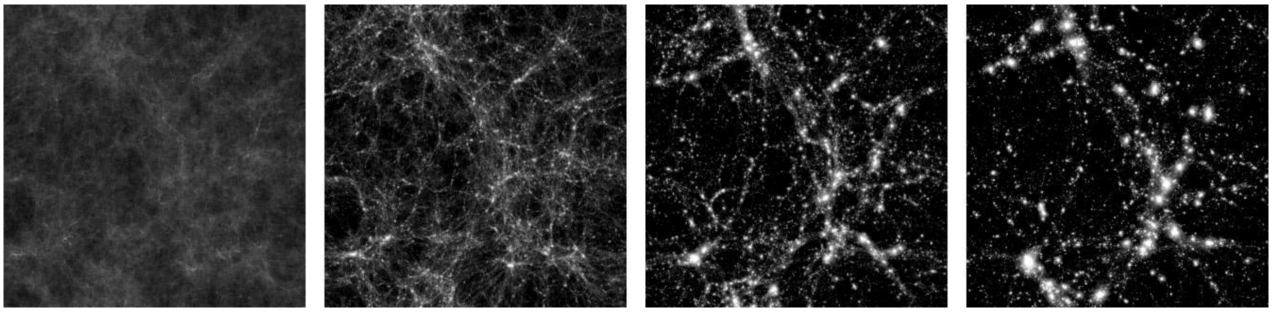

Figure 1: Time sequence of structure formation in a hierarchical clustering universe, here for the so-called ΛCDM model. The four snapshots correspond (from left to right) to redshifts of 9, 3.5, 1 and 0, respectively. The side length of the simulation box is $32.5\,h^{-1}$Mpc comoving.

is accreted in a smooth fashion, it settles in rotationally supported disk-like structures in which gas is slowly transformed into stars. Mergers, however, transform disk-like structures into spheroids. The Hubble type of a galaxy is thus determined by a continuing sequence of destruction of disks by mergers, accompanied by the formation of spheroidal systems, followed by the reassembly of disks due to smooth accretion. This picture of a hierarchical origin of galaxy morphology has been schematically incorporated in so-called semianalytical galaxy formation models used to study the evolution of the galaxy population, but the validity has never been directly demonstrated.

In this report I will discuss how individual galaxies are built up in a hierarchical clustering universe and whether the detailed balance between smooth accretion and mergers can account for the observed variety in the morphology of galaxies. I will investigate whether the progenitors of numerically simulated present day field galaxies have properties similar to observed Lyman-break galaxies. In particular I address how major global properties such as luminosity, star formation rate and potential depth change with redshift, and whether the hypothesis can be confirmed that the progenitors of present day field galaxies mainly contribute to the lower end of the high–z luminosity function.

2 Simulation technique

The simulations presented in this review have been performed using GRAPESPH, a code that combines the Smoothed Particle Hydrodynamics (SPH) approach to numerical hydrodynamics with a direct summation N-body integrator optimized for the special-purpose hardware GRAPE (Steinmetz 1996). GRAPESPH is fully Lagrangian and highly adaptive in space and time through the use of individual particle smoothing lengths and timesteps. It is thus optimally suited to study the formation of highly non-linear systems such as individual galaxy systems in a cosmological context. The following physical processes have been incorporated: the self-gravity of gas, stars, and dark matter, a full $3D$ hydrodynamical treatment of the gas, and radiative and Compton cooling. A simple recipe accounts for transforming gas into stars and for incorporating the feedback of mass and energy into the gaseous component driven by evolving stars.

Star formation is modeled by creating new collisionless "star" particles in Jeans-unstable, collapsing regions at a rate given by $\dot{\varrho}_\star = c_\star \varrho_{\rm gas} / \max(\tau_{\rm cool}, \tau_{\rm dyn})$. Here $\varrho_{\rm gas}$ is the local gas density, $\tau_{\rm cool}$ and $\tau_{\rm dyn}$ are the local cooling and dynamical timescales, respectively, and $c_\star$ is a star formation "efficiency" parameter. After formation, "star" particles are only affected by gravitational forces, but they devolve energy to their surroundings in a crude attempt to mimic the energetic feedback from supernovae: 10^{49} erg (per $M_\odot$ of stars formed) are injected into the surrounding gas about 10^7 yr after their formation. This energy is invested mostly in raising the internal energy (temperature) of the gas, but a fraction f_v is invested in modifying the bulk motion of the gas surrounding star forming regions.

The star formation prescription invokes two free parameters, the star formation efficiency $c_\star$ and the fraction f_v of the supernova energy that is invested in modifying the bulk motion of the gas surrounding star forming regions. The star formation parameters are calibrated such that Kennicutt's (1998) relation between the HI surface density and the star formation rate per unit area (Schmidt's law) is reproduced in isolated galaxy test cases.

The cosmological model investigated is the currently favored flat CDM model with a non-zero cosmological constant (ΛCDM: $\Omega = 0.3$, $h = 0.65$, $\Omega_b = 0.0125\,h^{-2}$, and $\Lambda = 0.7$). As in all models of the cold dark matter family, structure grows hierarchically, i.e. systems of progressively larger mass merge and collapse to form newly virialized systems (see figure 1).

3 Formation of a galaxy in a hierarchy of mergers

Figure 2 illustrates the the major evolutionary stages of a galaxy in a hierarchically clustering universe. The figure also demonstrates the amount of detail with which at present the formation of galaxies can be simulated. Numerical simulations are now able to capture the main stages of galaxy formation, and to resolve their main morphological components. In particular the following phases can be identified:

- **Formation of first disks.** At $z \approx 4$ the first protogalactic clumps are numerically resolved (i.e. more than 500 particles per halo). Small disks (diameter ≈ 3 kpc) form near the centers of these clumps.

- **Mergers and bulge formation.** The protogalactic clumps frequently merge ($z \approx 3$) with objects of comparable size and mass. The small disks at the center are destroyed in this process and a central spheroidal component forms.

- **Regeneration of disks.** In the absence of major mergers, disk-like structures around the bulge regenerate from gas accreted both smoothly and through minor mergers ($z \approx 2$). These objects feature all the major dynamical components of a bright spiral galaxy like the Milky Way: a rotationally supported disk of young stars, a centrally concentrated bulge, and a stellar halo of older stars.

- **Minor mergers and the formation of rapidly rotating bars.** Tidal torques during the close encounter with a minor satellite (mass ratio $\approx 1:10$) can trigger the formation of a rapidly rotating bar in the disk. The bar pattern persists long after the disruption of the culpable satellite. The bar extends out to about 2.5 kpc and has a corotation radius of slightly less than 3 kpc, implying, in agreement with the few barred galaxies where this ratio has been measured (Debattista & Sellwood 1999), that the bar is "fast". The bar pattern is clearly visible for more than 30 orbital periods, a consequence of repeated triggering by orbiting satellites aided by the fact that the baryonic component dominates the central potential (75% of the mass within 3 kpc is in the disk). Although the process described here is likely not the only bar formation mechanism acting on real galaxies, the simulation shows nevertheless a direct link between the presence of a bar pattern and the existence of satellites that may act as tidal triggers.

- **Major mergers and the formation of elliptical galaxies.** Mergers between close to equal mass galaxies effectively destroy disks and give rise to the formation of an elliptical galaxy. Residual gas in the disk progenitors is effectively channeled to the center where it is

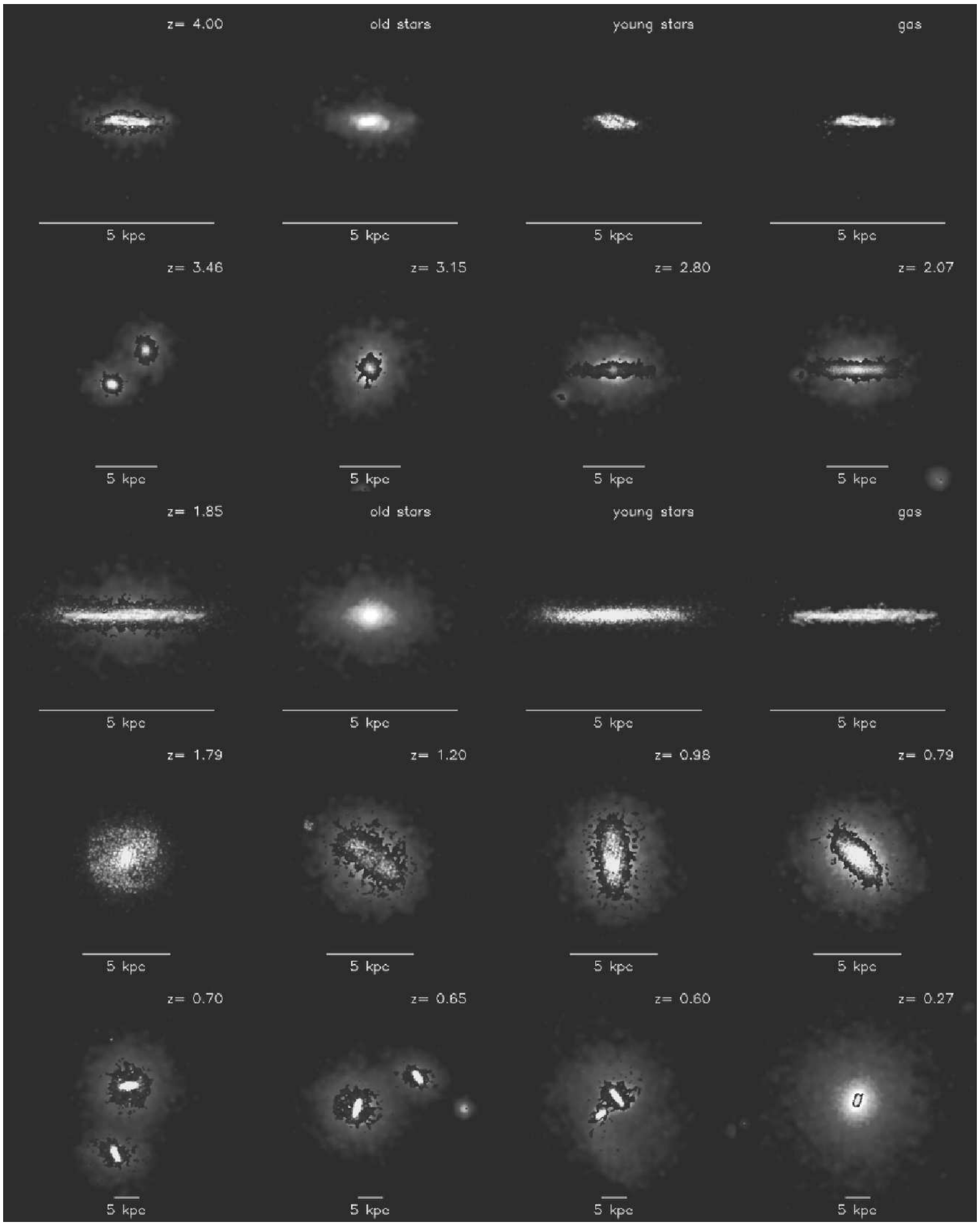

Figure 2: Surface density of the gaseous and stellar components of a LCDM halo at various epochs. Horizontal bars in each panel are 5 (physical) kpc long and indicate the scale of each figure. Rows 2, 4 and 5 show time sequences near some key evolutionary stage. Rows 1 and 3 decompose a galaxy at a particular redshift (left) into its constituents: old stars, young stars and gas (from left to right). Top row: The most massive progenitor at $z = 4$ shown edge-on. Second row: The formation of a bulge and the rebirth of a disk. Third row: The appearance of the galaxy at $z = 1.8$, seen edge-on. Fourth row: The tidal triggering of bar instability by a satellite resulting in the emergence of a rapidly rotating bar. Bottom row. A major merger and the formation of an elliptical galaxy.

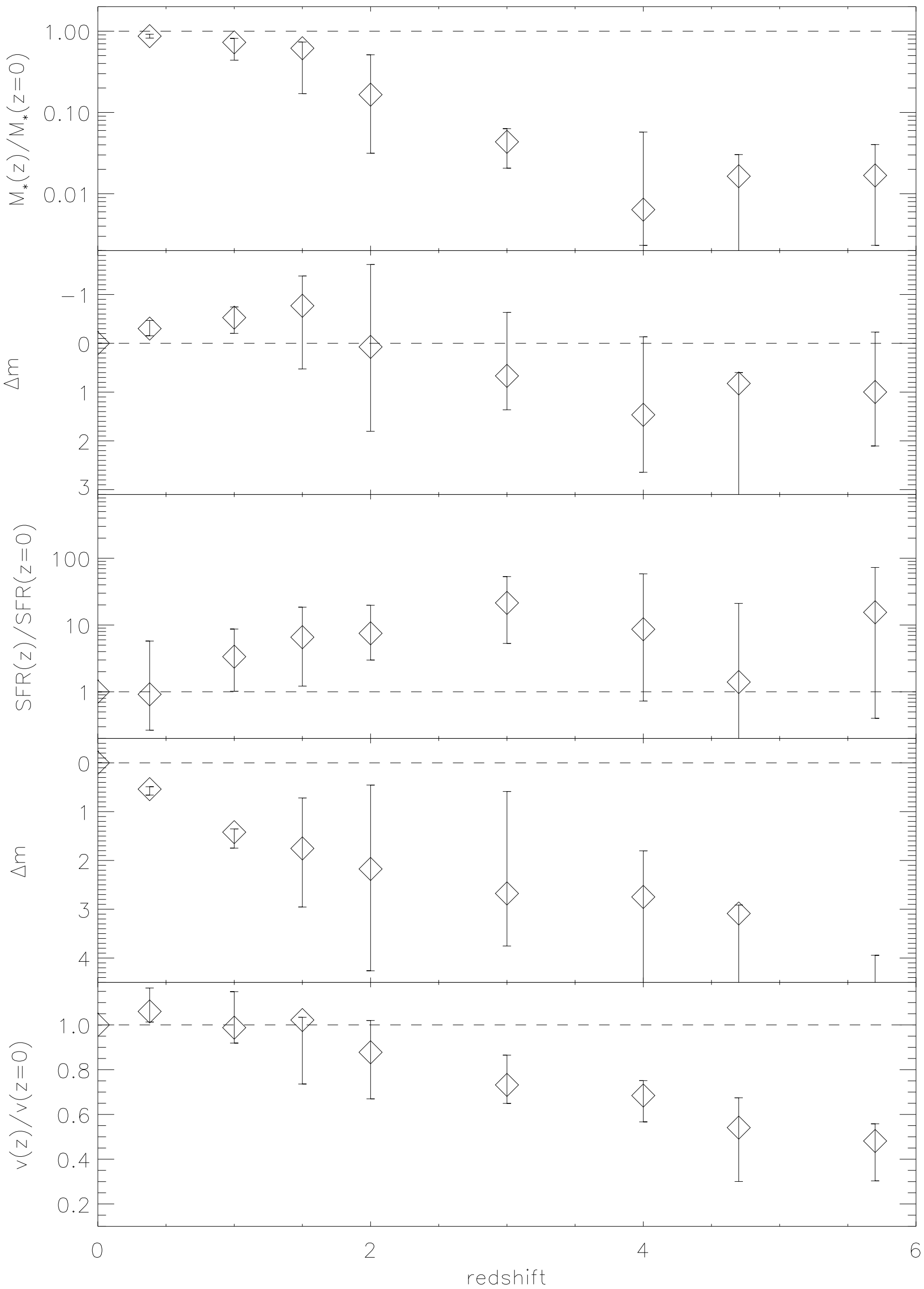

Figure 3: From top to bottom: (i) Stellar mass of the most luminous progenitor at redshift z normalized to the stellar mass of the present day galaxy. (ii) Magnitude difference in restframe R-band between the most luminous progenitor and the present day model galaxy. Effects of dust have not been taken into account. (iii) Star formation rate of the most luminous progenitor, normalized to its present day value. (iv) Difference in observed R-band between the most luminous progenitor and the present day model galaxy. (v) Ratio of circular velocity at 10 kpc of the most luminous progenitor and the present day galaxy. All error bars correspond to [20,80] percentile values.

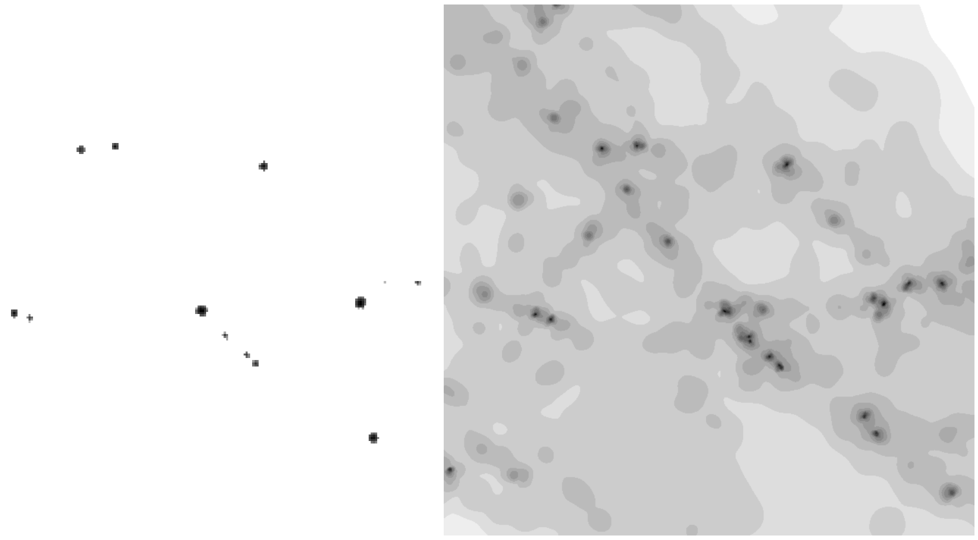

Figure 4: Left: Artificial R-band image of the $z = 3$ progenitors of a massive $z = 0$ galaxy in a HDF-like exposure. Right: H I column density map of a galaxy forming environment at redshift $z = 3$. Light gray corresponds to column densities of about $\log N = 13.5$, dark gray to $\log N \approx 15.5$ and black to $\log N > 17.5$. Each frame has a side length of 2.8 Mpc (comoving).

transformed to stars in a starburst like manner ($z = 0.25$). The resulting object is mainly composed of "old" stars with a sprinkle of young stars at the center that formed during the last major merger.

4 The properties of high redshift objects

In figure 3 the evolution of the stellar mass, magnitude, circular velocity and star formation rate of the most luminous progenitors of present day model galaxies is shown versus redshift. The top panel shows the ratio between the stellar mass of the most luminous progenitor and the present day model galaxy. The stellar mass of the most luminous progenitor has decreased to about 5–10% of its $z = 0$ value at redshift 3. Over the same time interval, the restframe R band absolute magnitude increases somewhat at lower redshift ($z \lesssim 1$) followed by a decline for higher redshifts ($z \gtrsim 1$). Out to a redshift of $z \approx 3$, changes are only moderate ($\lesssim$ 1mag), consistent with our earlier findings (Steinmetz & Navarro, 1999): As redshift increases, the decreasing mass of the most luminous progenitor is almost compensated by the combination of a lower mass–to–light ratio of the younger stellar population and a higher star formation rate (third panel).

In the fourth panel of figure 3, k-correction and dust absorption have been taken into account. While the intrinsic magnitudes increase as the UV light of star forming galaxies is redshifted into the R-band, the increased dust absorption at shorter wavelength more than compensates this effect, resulting in galaxies that are about 2.5 magnitudes dimmer at redshift 3. If the formation scenario described by this model is typical for the formation history of the Milky Way, these results imply that the most luminous progenitor of the Milky Way has an apparent magnitude of $m_R \approx 27.5$, two magnitudes dimmer than the current spectroscopic limit of Lyman-break galaxies.

The bottom panel of figure 3 depicts the evolution of the circular velocity of the model galaxies, measured at a radius of $r = 10\,\mathrm{kpc}$. Again little evolution can be seen out to redshift 5, the typical circular velocity at redshift 3 being still about 75% of its present day value with very

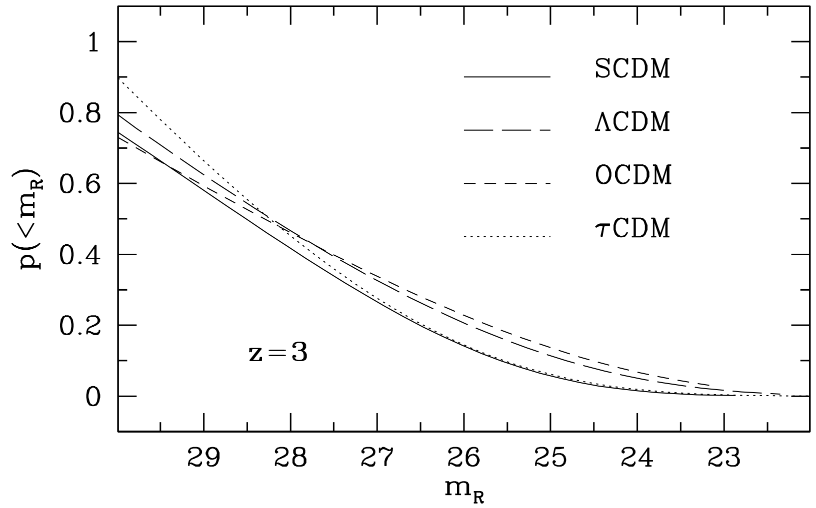

Figure 5: Predicted luminosity distribution for damped Lyα absorption systems for four different cosmologies

little difference between the cosmological scenarios. The combination of moderate evolution in magnitude and velocity results in only little evolution of the Tully–Fisher relation out to redshift one (Steinmetz & Navarro 1999, Mao, Mo and White, 1998), consistent with recent observational studies (e.g. Vogt et al. 1997).

5 The relation between high redshift galaxies and damped Lyman-α absorption systems

A generic prediction of any hierarchical cosmology is that a present day galaxy should have several progenitors at high redshift. This is illustrated in the left panel of figure 4. It shows the $z = 3$ progenitors of a $z = 0$ galaxy like the Milky Way ($v_c \approx 220\,\mathrm{km\,s^{-1}}$) in an artificial R-band image. The R-band image includes noise, PSF and exposure time similar to that of the Hubble Deep Field, but no absorption due to dust has been taken into account (see discussion below). The artificial image shows about 12 detectable objects (proto galactic clumps (PGCs)) that later on will merge to form the $z = 0$ galaxy. The separation of these PGCs is several hundred (physical) kpc and they are approaching each other at velocities of $\approx 200\,\mathrm{km\,s^{-1}}$.

The right hand side of figure 4 compares the distribution of stars in the PGCs with the distribution of HI. The gray scale corresponds to the HI column density. The lowest column density systems ($\log N(\mathrm{HI}) \approx 12 - 14$) are shown in light gray. They arise from gas in voids and sheets of the "cosmic web". Systems of higher column density are produced by filaments ($\log N \approx 14 - 17$, dark gray) or even gas that has cooled and that has collapsed in virialized halos ($\log N > 17$, black). In fact, HI distributions like the one shown in figure 4 are capable of explaining many properties of Lyα absorption systems (for details see, e.g., Cen et al. 1994; Katz et al. 1996; Zhang et al. 1995; Rauch, Haehnelt & Steinmetz 1997).

Figure 4 also unravels a close connection between PGCs and the regions of high column density. Each of the PGCs shown in the left panel is situated close to a region of very high column density ($\log N > 17$). However, there are still a substantial number of Ly-limit and damped Lyα systems (DLASs) that do not host sufficiently luminous stellar PGCs.

Do these PGCs correspond to the observed population of so-called Lyman-break galaxies (LBGs)? An analysis of the $z = 3$ progenitors of a set of simulated $z = 0$ galaxies with circular velocities of $\approx 200\,\mathrm{km\,s^{-1}}$ reveals that about one third of the progenitors are brighter than $m_R = 25.5$, the spectroscopic limit of current UV dropout surveys, but PGCs only occasionally are brighter than $m_R = 24$. This analysis however ignores the effect of dust. Current observational constraints favor a dust obscuration by ≈ 1.5 mag in R (1500Å restframe; Steidel et al. 2001), i.e., only a small fraction of progenitors exceeds the spectroscopic limit of $m_R = 25.5$. Similar conclusions have been drawn from the clustering of LBGs (Baugh et al. 1998), indicating that LBGs are the progenitors of the massive galaxies which, at $z = 0$, are located in galaxy clusters while the progenitors of typical field and group galaxies such as the Milky Way fall below the magnitude limit of about $m_R = 25.5$ (see however, Somerville et al. 2001).

A direct quantitative confirmation of this interpretation requires a numerical simulation that simultaneously covers sufficiently large cosmological volumes and resolves individual galaxy systems. These conditions cannot be matched by the currently available supercomputers. However, a hybrid scheme that combines the results of high resolution galaxy formation simulation with a Press-Schechter approach in order to predict the abundances of objects of a given circular velocity can give some further insight (Haehnelt et al. 2000). This model employs the close connection illustrated in figure 4 between the stellar PGCs and regions of sufficient HI column density to produce damped Lyα absorption. The hybrid model is calibrated to match simultaneously the observed abundances of LBGs and the overall rate of incidence, $d\mathcal{N}/dz = 0.2$. The result is shown in figure 5 for four different cosmological models (for details, see Haehnelt et al. 2000). More than 80% of the protogalactic clumps at redshift three which are capable of producing damped Lyα absorption fall above the magnitude limit of spectroscopic surveys, i.e. they are too dim to be identified with the population of Lyman break galaxies, consistent with the findings presented above. This result depends only weakly on the cosmological parameters. The rather faint flux levels also quite naturally explain why searches for the emission of DLAS have had only limited success (e.g.Møller & Warren 1998).

6 Summary

I described recent results modeling the formation and evolution of galaxies using high resolution gasdynamical simulations that include star formation and feedback processes. Application of these simulations to the properties of low and high redshift galaxies gave the following results:

- High resolution numerical simulation of individual galaxy systems provide clear support for the long-held view that the Hubble sequence can be understood in terms of accretion and merger histories and that morphology may be a transient phenomenon in the lifetime of a galaxy. Most of the stars that make up the halo and bulge of disk galaxies may have been born in early proto-disks that were later stirred into spheroids by mergers.

- A typical $z = 0$ field galaxy has several progenitors at redshift $z = 3$. These progenitors are spread over a volume with a diameter of several hundred kpc.

- At $z = 3$, the most luminous progenitor has a rest frame luminosity about 1 mag dimmer than its present day counterpart and circular velocity of about 75% of its present day value. Star formation rates are about a factor of 2–20 higher than at the present day.

- Only the brightest galaxies have a progenitor brighter than $m_R = 25.5$, i.e. bright enough to be included in current spectroscopically confirmed samples of UV dropout galaxies. The majority of the progenitors have $m_R > 25.5$, in particular if dust obscuration is taken into account.

- Only about 10% to 20% of DLASs are predicted to be brighter than $m_R = 25.5$. The rather faint flux levels and small impact parameters predicted for the majority of DLASs explain why searches for the emission from DLASs have been notoriously difficult.

Although the progenitors of numerically simulated present day galaxies in the CDM scenario have many properties similar to those of Lyman-break galaxies, they are on average too dim to be identified with spectroscopically confirmed LBGs. The simulations thus support a picture that envisions LBGs as the progenitors of massive galaxies as they can be found in present day galaxy clusters.

Acknowledgements: This work has been supported by the National Aeronautics and Space Administration under NASA grant NAG 5-7151, by the National Science Foundation under NSF grant 9807151, and by fellowships from the Alfred P. Sloan Foundation and the David and Lucile Packard foundation. This article includes work from collaborations with V. Eke, M. Haehnelt, J. Navarro and M. Rauch.

References

Baugh, C.M., Cole, S., Frenk, C.S., Lacey, C.G. 1998, ApJ, 498, 504.
Bouwens, R., Broadhurst, T., Silk, J. 1998, ApJ, 506, 557
Cen, R., Miralda-Escudé, J., Ostriker, J.P., Rauch, M. 1994, ApJ, 437, L9
Contardo, G., Steinmetz, M., Fritze-von Alvensleben, U. 1998, ApJ, 507, 497
Debattista, V.P., Sellwood, J. 1999, ApJ, 493, L5.
Haehnelt, M., Steinmetz, M., Rauch, M. 2000, ApJ, 534, 594.
Katz, N., Weinberg, D. H., Hernquist, L. 1999, ApJ, 423, 463.
Katz, N., Weinberg, D. H., Hernquist, L., Miralda-Escudè J. 1996, ApJ, 457, L57
Kauffmann, G., Colberg, J.M., Diaferio, A., White, S.D.M. 1999, MNRAS, 307, 529.
Kennicutt, R.C. 1998, ARA&A, 36, 189.
Mao, S., Mo, H.J., White, S.D.M. 1998, MNRAS, 297, L71.
Mo, H.J., Fukushita, M. 1996, ApJ, 467, L9
Møller, P., Warren, S.J. 1998, MNRAS, 299, 661.
Pearce, F.R., Jenkins, A., Frenk, C.S., Colberg, J.M., White, S.D.M., Thomas, P.A., Couchman, H.M.P., Peacock, J.A., Efstathiou, G. 1999, ApJ, 521, 99.
Rauch, M., Haehnelt, M.G., Steinmetz, M. 1997, ApJ, 481, 601.
Somerville, R.S., Primack, J.R., Faber, S.M. 2001, MNRAS, 320, 504.
Steidel C. C., Giavalisco M., Pettini M., Dickinson M., Adelberger K. L. 1996, ApJ, 462, L49 Steidel, C.C., Pettini, M., Adelberger, K.L. 2001, ApJ, 546, 665
Steinmetz, M. 1996, MNRAS, 278, 1005
Steinmetz, M., Navarro, J.F. 1999, ApJ, 513, 555.
Vogt, N.P., Phillips, A.C., Faber, S.M., Gallego, J., Gronwall, C., Guzmán, R., Illingworth, G.D., Koo, D.C., Lowenthal, J.D. 1997, ApJ, 479, L121
Zhang Y., Anninos P., Norman M.L. 1995, ApJ, 453, L57